THE JOURNAL OF BIOLOGICAL CHEMISTRY VOL. 283, NO. 42, pp. 28321–28328, October 17, 2008

Lysyl-tRNA Synthetase Is a Target for Mutant SOD1 Toxicity in Mitochondria*

Received for publication, July 22, 2008, and in revised form, August 18, 2008 Published, JBC Papers in Press, August 20, 2008, DOI 10.1074/jbc.M805599200

Hibiki Kawamata[‡], Jordi Magrané[‡], Catherine Kunst[§], Michael P. King[¶], and Giovanni Manfredi[‡1]

From the [‡]Department of Neurology and Neuroscience, Weill Medical College of Cornell University, New York, New York 10065, the [§]Eleanor Roosevelt Institute, University of Denver, Denver, Colorado 80206, and the [¶]Department of Biochemistry and Molecular Pharmacology, Thomas Jefferson University, Philadelphia, Pennsylvania 19107

Amyotrophic lateral sclerosis (ALS) is a devastating neurodegenerative disease affecting the motor neurons. The majority of familial forms of ALS are caused by mutations in the Cu,Zn-superoxide dismutase (SOD1). In mutant SOD1 spinal cord motor neurons, mitochondria develop abnormal morphology, bioenergetic defects, and degeneration. However, the mechanisms of mitochondrial toxicity are still unclear. One possibility is that mutant SOD1 establishes aberrant interactions with nuclear-encoded mitochondrial proteins, which can interfere with their normal trafficking from the cytosol to mitochondria. Lysyl-tRNA synthetase (KARS), an enzyme required for protein translation that was shown to interact with mutant SOD1 in yeast, is a good candidate as a target for interaction with mutant SOD1 at the mitochondrion in mammals because of its dual cytosolic and mitochondrial localization. Here, we show that in mammalian cells mutant SOD1 interacts preferentially with the mitochondrial form of KARS (mitoKARS). KARS-SOD1 interactions occur also in the mitochondria of the nervous system in transgenic mice. In the presence of mutant SOD1, mitoKARS displays a high propensity to misfold and aggregate prior to its import into mitochondria, becoming a target for proteasome degradation. Impaired mitoKARS import correlates with decreased mitochondrial protein synthesis. Ultimately, the abnormal interactions between mutant SOD1 and mitoKARS result in mitochondrial morphological abnormalities and cell toxicity. mitoKARS is the first described member of a group of mitochondrial proteins whose interaction with mutant SOD1 contributes to mitochondrial dysfunction in ALS.

Amyotrophic lateral sclerosis (ALS)[2] is a progressive neurodegenerative disorder of motor neurons that results in paralysis and death within five years of diagnosis. Approximately 10% of ALS cases are inherited, of which 20% are associated with mutations in the Cu,Zn-superoxide dismutase, SOD1.

SOD1 is a free radical scavenging enzyme, but because many SOD1 mutations do not affect the enzymatic activity and the disease has an autosomal dominant transmission, a toxic gain of function of the mutant protein has been postulated. SOD1 is abundantly expressed in the cytosol, but a proportion of mutant SOD1 is also associated with mitochondria, where its aggregation could have pathological consequences (1–7). Transgenic mice expressing mutant human SOD1 (hSOD1) develop mitochondrial degeneration in motor neurons (8, 9), whose appearance coincides with the onset of symptoms (10). Furthermore, mutant hSOD1 transgenic mice develop dysfunction of mitochondrial respiration and ATP synthesis (4, 11, 12). In addition, we have demonstrated that this bioenergetic failure results in impaired mitochondrial calcium uptake in the spinal cord and brain of mutant hSOD1 mice (13). Despite the evidence that mutant SOD1 causes mitochondrial dysfunction (14), the molecular mechanisms underlying the mitochondrial damage remain to be identified.

The large majority of mitochondrial protein components are nuclear-encoded, synthesized in the cytosol, and imported into mitochondria through specialized import machineries. Thus, one hypothesis for mutant SOD1 toxicity involves aberrant interactions of mutant SOD1 with mitochondrial proteins (7), resulting in disruption of their normal folding and import (3). Interactions involving mutant SOD1 have been reported with proteins that may affect directly or indirectly mitochondria, including heat shock proteins and Bcl-2 (15, 16). In a yeast two-hybrid screen, lysyl-tRNA synthetase (KARS), an enzyme required for protein synthesis, was found to interact with mutant but not with wild type (WT) SOD1 (17). KARS is a potential candidate for abnormal interactions with SOD1 affecting mitochondria, because it exists both as a cytosolic (cytoKARS) and as a mitochondrially imported (mitoKARS) enzyme.

Here, we investigate the interactions between mutant hSOD1 and KARS in mammalian cells and their consequences on mitochondrial integrity and cell viability. We find that as a consequence of aberrant interactions with mutant hSOD1, mitoKARS misfolds prior to or during its import into mitochondria and becomes targeted for proteasomal degradation.

* This work was supported, in whole or in part, by National Institutes of Health Grants P01-NS011766, R01-NS051419, and F31 NS054554. This work was also supported by the Robert Packard ALS Research Center, The New York Community Trust, and the Muscular Dystrophy Association.

[1] To whom correspondence should be addressed: Weill Medical College of Cornell University, 525 East 68th St., A-505, New York, NY 10065. Tel.: 212-746-4605; Fax: 212-746-8276; E-mail: gim2004@med.cornell.edu.

[2] The abbreviations used are: ALS, amyotrophic lateral sclerosis; SOD1, Cu,Zn-superoxide dismutase; hSOD1, human SOD1; KARS or LysRS, lysyl-tRNA synthetase; mitoKARS, mitochondrial lysyl-tRNA synthetase; cytoKARS, cytosolic lysyl-tRNA synthetase; pre-MSK1p, yeast mitoKARS precursor; mitoGFP, mitochondrially targeted green fluorescent protein; GAPDH, glyceraldehyde-3-phosphate dehydrogenase; Tim23, translocase of inner membrane 23-kDa subunit; Hsp70, heat shock protein 70; MnSOD, manganese-superoxide dismutase; PBS, phosphate-buffered saline; WT, wild type; IP, immunoprecipitation; co-IP, co-immunoprecipitation; UPS, ubiquitin-proteasome system; mtDNA, mitochondrial DNA.

Mutant hSOD1-mitoKARS interactions result in the formation of high molecular weight protein aggregates that correlate with impaired mtDNA-encoded protein synthesis, mitochondrial morphological abnormalities, and decreased cell survival.

EXPERIMENTAL PROCEDURES

Expression Plasmids—Human mitoKARS cDNA was cloned in pEF/Myc/cyto (Invitrogen) as described previously (18). Human cytoKARS with a C-terminal FLAG epitope tag and hSOD1 cDNAs (wild type and G93A and G85R mutants) were cloned into pCIneo (Promega, Madison, WI) and pcDNA3.0 (Invitrogen), respectively. Mitochondrial GFP (mitoGFP) was a gift of Dr. Rosario Rizzuto (19) (University of Ferrara, Ferrara, Italy).

Cell Culture, Transfection, and Proteasome Inhibition—COS-7 cells (ATCC, Manassas, VA) were cultured in advanced Dulbecco's modified Eagle's medium (Invitrogen) supplemented with 2% fetal bovine serum (Cellgro, Herndon, VA) and Gluta-max (Invitrogen), in 5% CO_2 at 37 °C.

Transfections with plasmids encoding KARS and hSOD1, either individually or in combination, were performed using FuGENE 6 transfection reagent (Roche Applied Science) according to the manufacturer's instructions. For proteasome inhibition experiments, the cells were treated for 16 h with 20 μM (complete inhibition) or 75 nM (partial inhibition) of MG132 (Sigma).

hSOD1 Transgenic Mice—Transgenic mice expressing WT (N1029) or G93A (20) hSOD1 were obtained from the Jackson Laboratory (Bar Harbor, ME) and bred at the Weill Medical College of Cornell University animal facility. All of the animal procedures were approved by the Animal Care and Use Committee of the Weill Medical College of Cornell University.

Cell Imaging by Immunocytochemistry—Forty-eight hours post-transfection, the cells grown on glass coverslips were washed in phosphate-buffered saline (PBS) and fixed in 4% paraformaldehyde. After three washes in PBS, the cells were permeabilized with 0.1% Triton X-100, and blocked in PBS containing 1% bovine serum albumin and 10% normal goat serum. The cells were incubated with primary antibodies diluted in blocking buffer for 2 h with gentle agitation. Fluorescently labeled secondary antibodies were diluted in blocking buffer and applied to cells for 1 h. The cells were washed in PBS three times after primary and secondary antibody incubations. All of the steps were performed at room temperature.

The following antibodies were used: monoclonal hSOD1 (Santa Cruz Biotechnology, Santa Cruz, CA), polyclonal SOD1 (Stressgen, Victoria, Canada), FLAG-M2 (Sigma), monoclonal Myc (Upstate, Lake Placid, NY or Abcam, Cambridge, MA), polyclonal Myc (Sigma), Hsp70 (Stressgen), and MnSOD (Stressgen).

Immunostained cells were imaged with a Zeiss LSM 510 laser scanning confocal microscope with a 63× Plan Apochromat oil immersion lens with aperture 1.4 using a photomultiplier (Carl Zeiss MicroImaging, Inc.). A series of *z* sections were taken spanning the thickness of the cell with intervals between sections set at 0.5 μm. *z* stack images were projected onto a single plane using the LSM Image Browser software (Carl Zeiss MicroImaging, Inc.), and digital magnification was 2× (total magnification was 126×).

Cell Viability Assay—COS cells grown in 48-well plates were transfected with hSOD1 (WT, G93A, G85R, or empty vector) with or without mitoKARS. Twenty-four hours later, the cells were washed once in PBS and incubated with 2.5 μM calcein AM (Invitrogen) for 10 min at room temperature. Fluorescence was measured at 485-nm excitation and 535-nm emission in an HTS 7000 plus plate reader (Packard Instrument Company, Downers Grove, IL) with background subtraction.

Cell and Tissue Fractionation—COS cells transfected with hSOD1 and KARS were fractionated into cytosolic and enriched mitochondrial fractions according to established protocols (21). Mouse brain and spinal cord mitochondria were isolated and purified in a Ficoll gradient as described previously (6) with minor modifications. The tissue homogenization buffer contained 20 mM Hepes instead of Tris-HCl to allow for chemical cross-linking.

Immunoprecipitation and Western Blot Analyses—Cells or tissue fractions were cross-linked with 2 mM dithiobis(succinimidyl propionate) (Pierce) dissolved in Me_2SO for 30 min at room temperature, followed by the addition of 20 mM Tris (pH 7.6) and incubation for 15 min to stop the reaction. For cells, the samples were washed three times in PBS, lysed in RIPA buffer containing 20 mM Tris, pH 7.4, 150 mM NaCl, 1% Triton X-100, 1% sodium deoxycholate, 0.1% sodium dodecyl sulfate, and a protease inhibitor mixture (Roche), and cleared by centrifugation at 10,000 × *g* for 5 min at 4 °C. The supernatants were incubated overnight at 4 °C with protein G-Sepharose beads (Zymed Laboratories Inc., S. San Francisco, CA), which had been preadsorbed with appropriate antibodies for 2 h at room temperature and collected by brief centrifugation. The following day, the beads were washed three times in RIPA buffer and boiled for 10 min in Laemmli buffer containing 50 mM dithiothreitol prior to electrophoresis. For mouse tissue, the samples were solubilized with 1% Triton X-100 for 15 min at room temperature. Immunoprecipitation was performed as above, except that the buffer contained 10 mM Tris, pH 7.4, 320 mM sucrose, 150 mM NaCl, 5 mM $MgCl_2$, and 1% Triton X-100.

Immunoprecipitated samples were separated by standard SDS-polyacrylamide gel electrophoresis. The proteins were transferred to polyvinylidene difluoride membranes (Bio-Rad). The membranes were blocked in 5% milk (in Tris-buffered saline with 0.1% Tween 20) for 1 h, followed by primary antibody incubation overnight at 4 °C. Horseradish peroxidase-conjugated secondary antibodies were applied for 1 h at room temperature, and immunoreactive bands were revealed with the enhanced chemiluminescence reagent (Pierce). The following antibodies were used for immunoprecipitation and detection of proteins: LysRS against human KARS (22), polyclonal SOD1 (Calbiochem, La Jolla, CA), ubiquitin (Chemicon Millipore, Billerica, MA), glyceraldehyde-3-phosphate dehydrogenase (GAPDH, Abcam), Tim23 (BD Biosciences, La Jolla, CA), Myc, and FLAG-M2.

Blue Native Gel Electrophoresis—COS cells were transfected with mitoKARS with or without hSOD1 (WT, G93A, and G85R). The mitochondria were solubilized, and native protein complexes were separated by blue native gel electrophoresis

and transferred to polyvinylidene difluoride membranes, as described previously (23). The membranes were blocked in 5% milk in Tris-buffered saline-Tween for 8 h and immunoprobed with LysRS or complex III core II subunit (Invitrogen) antibodies.

Filter Trap Assays—The filter trap assay was described previously (6). Briefly, cytosolic and mitochondrial fractions from COS cells or tissues were incubated with 0.5% Triton X-100 for 15 min on ice. The samples were vacuum-filtered through 0.22-μm cellulose acetate membranes (GE Osmonics, Trevose, PA) using a 96-well dot blot apparatus (Bio-Rad). The membranes were washed and immunodetected with appropriate primary and secondary antibodies as described above. In a set of experiments, proteinase K treatment was performed on mitochondrial fractions from COS cells co-transfected with mutant hSOD1 and mitoKARS prior to performing the filter trap assay. Twenty μg of the samples were treated with 20 μg/ml proteinase K on ice for 30 min. Proteinase K was inactivated with 2 mM phenylmethanesulfonyl fluoride for 15 min.

Mitochondrial Protein Synthesis Analysis—The rate of mitochondrial protein synthesis was measured by pulse-labeling experiments with [^{35}S]methionine according to the method of Chomyn (24). COS cells were co-transfected with WT or G85R hSOD1 and mitoKARS. 48 h post-transfection, the cells were labeled with [^{35}S]methionine (0.2 mCi of 1,175 Ci/mmol/plate) for 30 min in the presence of the cytoplasmic translation inhibitor emetine (50 μg/ml). The labeled cells were trypsinized, washed, and treated with 1% SDS. Samples containing 50 μg of protein were electrophoresed through a 15–20% exponential SDS-polyacrylamide gradient gel. The gel was dried and exposed to a phosphorimaging screen, and selected radioactive bands corresponding to mtDNA-encoded peptides ND5, ND1, and A6 were analyzed with a Cyclone phosphorimaging device (Packard Instrument Company).

Cell lysates were also subjected to Western blot to determine the expression levels of mitoKARS and hSOD1 using antibodies against Myc and SOD1, as well as loading controls for nuclear-encoded mitochondrial protein, Tim23, and the cytosolic protein, GAPDH.

RESULTS

KARS Expression and Subcellular Localization in COS Cells—Expression studies with the two isoforms of KARS were conducted using plasmid vectors coding for human mitoKARS or cytoKARS tagged at the C-termini with Myc and FLAG epitopes, respectively (Fig. 1*A*). Upon transient transfection in COS cells, mitoKARS is distributed to the mitochondria, as shown by co-localization of Myc immunostaining with the mitochondrial matrix protein MnSOD (Fig. 1*B*). In contrast, the cytoKARS protein lacking a mitochondrial targeting signal is expressed diffusely in the cell and co-localizes with the cytoplasmic chaperone protein, Hsp70 (Fig. 1*C*).

Subcellular localization of KARS was further analyzed by immunoblot of cytosolic and mitochondrial fractions. mitoKARS is detected as the 69-kDa unprocessed form (*i.e.* still containing the N-terminal mitochondrial targeting signal) in the cytosolic fraction and predominantly as the 64-kDa processed form in the mitochondrial fraction (Fig. 1*D*). As

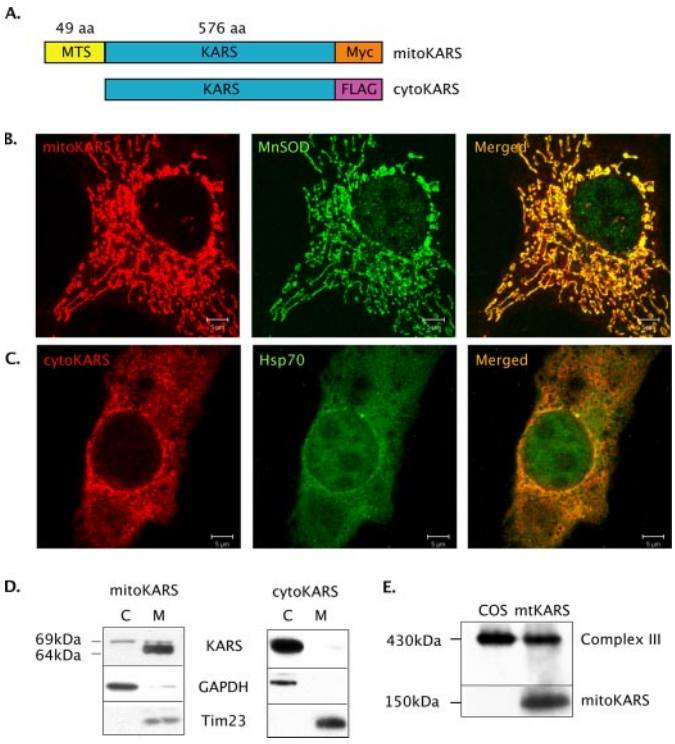

FIGURE 1. **KARS expression and localization in COS cells.** *A*, diagram of KARS expression constructs. The mitoKARS construct contains a 49-amino acid N-terminal cleavable mitochondrial targeting sequence (*MTS*). cytoKARS and mitoKARS are epitope-tagged at the C-termini with FLAG and Myc, respectively. *B*, COS cells transiently transfected with mitoKARS and analyzed by immunocytochemistry. Immunostaining for mitoKARS with Myc (in *red*) and with the mitochondrial matrix protein, MnSOD (in *green*) show mitochondrial co-localization (*yellow* in the merged image). *C*, cytoKARS detected with FLAG antibody (in *red*) and the cytosolic protein Hsp70 (in *green*) show diffuse intracellular expression and co-localization (*yellow* in the merged image). *D*, a Western blot of subcellular fractions with Myc antibody (*left panel*) shows the unprocessed (69-kDa band) and the processed (64-kDa band) mitoKARS in the cytosol (*lanes C*) and the mitochondria (*lanes M*), respectively. cytoKARs detected with FLAG (*right panel*) is exclusively localized in the cytosol. GAPDH and Tim23 are markers of the cytosolic and mitochondrial contents, respectively. *E*, blue native gel analysis with LysRS antibody shows a 150-kDa band in mitoKARS-expressing cells, presumably corresponding to a protein dimer. Complex III of the respiratory chain was used to confirm the native state of mitochondrial protein complexes.

expected, cytoKARS is localized only in the cytosolic fraction (Fig. 1*D*). Glyceraldehyde-3-phosphate dehydrogenase (GAPDH) and Tim23 were used as the cytosolic and mitochondrial markers, respectively.

cytoKARS is thought to form a dimer, which is part of a large protein complex containing multiple aminoacylating enzymes (25, 26), but the functional structure of mitoKARS has not yet been defined. Thus, to assess whether also mitoKARS exists in multimeric complexes, we performed a blue native gel analysis, which detected a single band of ~150 kDa, presumably corresponding to a mitoKARS dimer (Fig. 1*E*).

mitoKARS Co-immunoprecipitates with SOD1—Co-immunoprecipitation (co-IP) experiments were carried out to investigate the interaction between hSOD1 and mitoKARS. Because KARS was shown to interact with mutant SOD1 in yeast (17), we tested two different mutants of hSOD1, G93A and G85R, and compared them with WT hSOD1. The two mutants differ by their structural and biochemical properties, because the G93A hSOD1 is folded into a stable and active protein, whereas

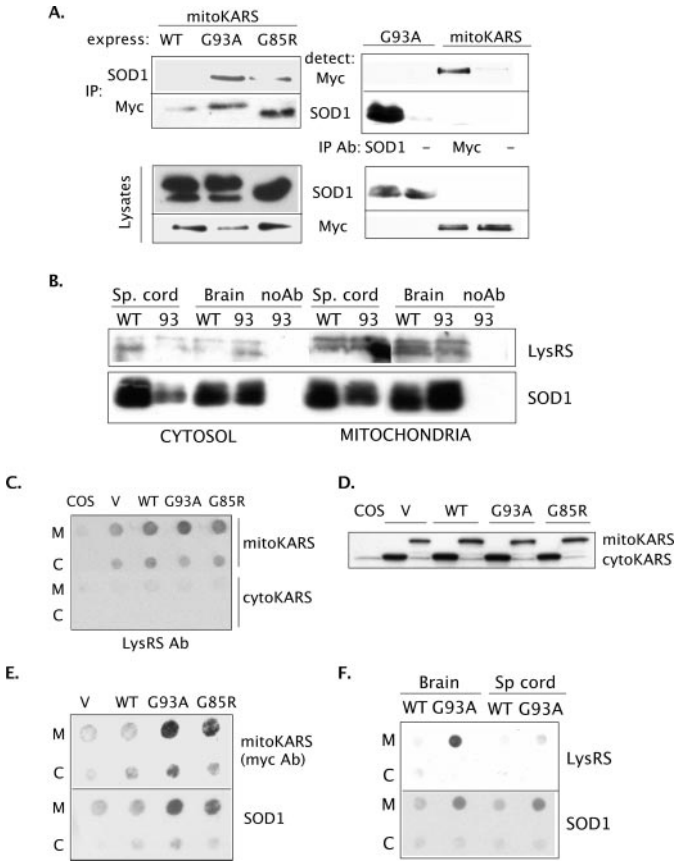

FIGURE 2. **mitoKARS-hSOD1 interaction and aggregation.** *A*, *left panel*, COS cells were transiently transfected with hSOD1 (WT, G93A, or G85R) and mitoKARS. IP on total cell lysates was performed using either polyclonal SOD1 or Myc antibodies. Proteins immunoprecipitated by SOD1 were detected with antibodies against Myc and *vice versa*. Expression levels of hSOD1 and mitoKARS are shown in the *bottom left panel*. *Right panel*, control for IP specificity performed with and without primary antibodies (*Ab*). *B*, *top panel*, Co-IP of KARS with SOD1 antibody on cytosolic and enriched mitochondrial fractions from 60 days old transgenic mouse brains and spinal cords was detected with the LysRS antibody. *Bottom panel*, IP of SOD1 detected with the SOD1 antibody on the same blot as in the *top panel*. As expected, negative controls without primary anti SOD1 antibody do not pull down either KARS or SOD1. *C*, filter trap assay on 10 μg of cytosolic (*row C*) and mitochondrial (*row M*) proteins from COS cells co-transfected with hSOD1 or empty vector (*V*) and either cytoKARS or mitoKARS. The membrane was probed with LysRS antibody. *D*, KARS expression levels detected by LysRS in lysates from cells used in *C*. *E*, filter trap assay on 50 μg of cytosolic (*row C*) and mitochondrial (*row M*) fractions of COS cell co-transfected with hSOD1 or empty vector plus mitoKARS, detected with Myc or SOD1 antibodies. Mitochondria containing mutant hSOD1 aggregates also show higher levels of mitoKARS aggregates. *F*, *top panel*, a filter trap on 10 μg of mitochondrial (*row M*) and cytosolic (*row C*) proteins from brain and spinal cord of 60-day-old WT and G93A hSOD1 transgenic mice detected with the LysRS antibody shows KARS aggregates in the mitochondrial fractions of the G93A mice. *Bottom panel*, filter trap of the same samples as in the *top panel* probed with the SOD1 antibody.

the G85R hSOD1 is highly unstable and lacks detectable dismutase activity. mitoKARs is pulled down by the SOD1 antibody only in cells expressing mutant hSOD1. Reverse co-IP with the Myc antibody pulls down G93A and G85R mutant hSOD1 efficiently, whereas only a small amount of WT hSOD1 is detected (Fig. 2*A*, *top left panels*), despite the fact that similar amounts of the three forms of hSOD1 are expressed in cell lysates (Fig. 2*A*, *bottom left panels*). As expected, a negative control co-IP in the absence of antibodies failed to pull down KARS or SOD1 (Fig. 2*A*, *top right panels*). Under the same experimental conditions, expression of mutant or WT hSOD1 together with cytoKARS did not result in detectable co-IP of the two proteins (data not shown), suggesting that SOD1 interacts selectively with mitoKARS and not with cytoKARS.

To assess whether SOD1-KARS interactions take place *in vivo* in a disease-relevant tissue with endogenous expression of KARS, we investigated mitochondrial and cytosolic fractions from brain and spinal cord of WT and G93A hSOD1 transgenic mice. When SOD1 was pulled down, co-immunoprecipitated KARS was detected using the LysRS antibody, which recognizes both forms of KARS. This antibody was raised against human KARS (22), but it reacts also with mouse KARS. Both WT and G93A SOD1 pulled down endogenous KARS more efficiently in the mitochondrial fractions as compared with the cytosolic ones, both in brain and spinal cord (Fig. 2*B*). Relative to the amount of immunoprecipitated SOD1, KARS is pulled down more efficiently in G93A than in WT spinal cord mitochondria, suggesting that KARS may interact more strongly with mutant than WT hSOD1.

SOD1 Induces the Formation of Aggregates Containing mitoKARS—Mutant SOD1 forms aggregates in the cytosol and mitochondria (6, 27). Therefore, we hypothesized that aberrant protein-protein interaction with mutant SOD1 would lead to recruitment of KARS into aggregates. COS cells were co-transfected with WT or mutant hSOD1 and either cyto or mitoKARS and cytosolic and mitochondrial fractions were subjected to size exclusion filter trap assays. Using the LysRS antibody, we find that cells expressing mitoKARS contain unfilterable aggregates in the mitochondrial fraction. On the other hand, in both the cytosolic and mitochondrial fractions of cells transfected with cytoKARS, unfilterable aggregates are virtually undetectable (Fig. 2*C*). This is not due to lower expression of cytoKARS than mitoKARS, as shown by Western blot of the lysates (Fig. 2*D*). We note that the expression of mitoKARS alone results in aggregation (Fig. 2*C*), but co-expression with hSOD1 clearly increases mitoKARS aggregation. In the same mitoKARS and SOD1 transfected cell samples, we also confirm the presence of mitoKARS aggregates associated with mitochondria using the Myc antibody and show that mutant hSOD1 increases KARS aggregation more than WT hSOD1 (Fig. 2*E*). Filter trap assays of cytosolic and mitochondrial fractions from brain and spinal cord of transgenic mice show unfilterable protein aggregates containing KARS, which are more abundant in the mitochondrial fraction of G93A mice (Fig. 2*F*, *top panel*). These aggregates correlate with the presence of unfilterable SOD1 aggregates (Fig. 2*F*, *bottom panel*), indicating that also *in vivo* KARS aggregates are preferentially associated with mitochondria containing mutant hSOD1.

mitoKARs Aggregates Are Associated with the Outer Surface of Mitochondria—The presence of mitoKARS aggregates in the cytoplasmic fractions (Fig. 2, *C* and *E*) suggests that a portion of the protein aggregates prior to being imported. To determine the site of formation of the mitoKARS aggregates, we treated intact mitochondria with proteinase K prior to the filter trap assay. The majority of mitoKARS aggregates are digested by proteinase K, whereas MnSOD, a protein of the mitochondrial matrix, is protected from digestion (Fig. 3*A*), suggesting that

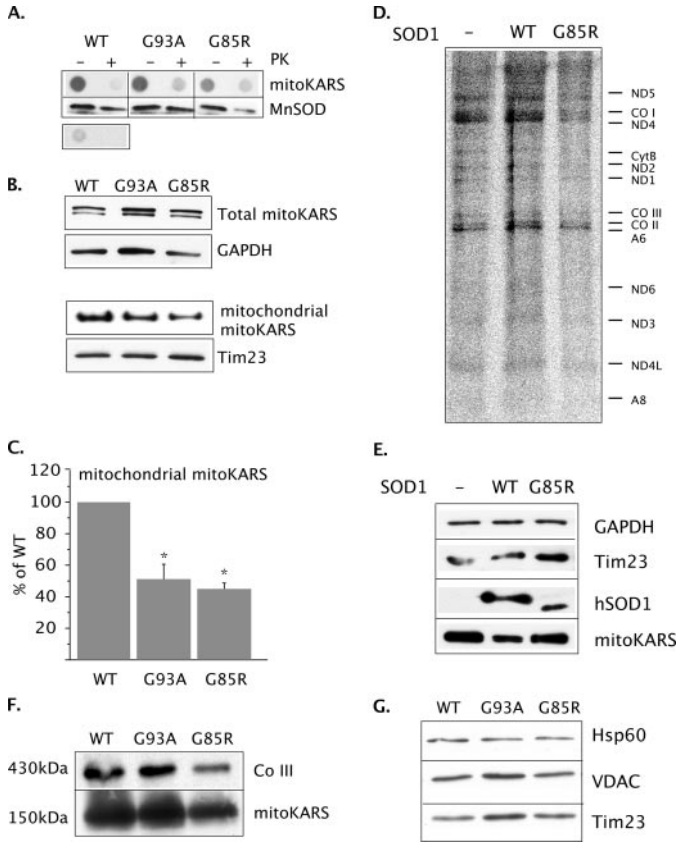

FIGURE 3. **Aggregation on the outer surface of mitochondria hinders mitoKARS import and mitochondrial protein synthesis.** *A*, *top panels*, filter trap on 20 μg of mitochondrial proteins from cells co-transfected with hSOD1 and mitoKARS, with or without proteinase K (*PK*) treatment. The WT blot was exposed longer than the mutants to detect low abundance aggregated mitoKARS in the PK treated sample. The lower exposure is shown below. *Bottom panels*, samples were probed for the matrix protein MnSOD to test mitochondrial integrity. *B*, COS cells were co-transfected with hSOD1 and mitoKARS. *Top panels*, total cellular contents of mitoKARS and GAPDH. *Bottom panels*, mitochondrial content of mitoKARS and Tim23. *C*, mitochondrial association of mitoKARS was quantified by densitometry of the Western blot bands shown in *B*. The amounts of mitoKARS in total lysates and mitochondrial fractions were normalized by GAPDH and Tim23, respectively. Then the amounts of mitochondrially associated mitoKARS were estimated as mitoKARS in the mitochondrial fraction over the total cellular mitoKARS. SOD1 mutant cells were compared with WT ones. The differences were determined by analysis of variance followed by Fisher's post-hoc test. *, $p < 0.05$, $n = 3$. The *error bars* indicate S.E. *D*, COS cells were transfected with mitoKARS and hSOD1 (WT or G85R), and mitochondrial protein synthesis rates were analyzed by metabolic labeling with [^{35}S]methionine in the presence of emetine. Equal amounts of proteins (50 μg) were separated on a SDS-15–20% exponential polyacrylamide gradient gel. *E*, Western blot of COS cell lysates from the mitochondrial protein translation experiment in *D*, probed with antibodies against GAPDH and Tim23 as loading controls for nuclear-encoded cytosolic and mitochondrial proteins, respectively. Expression of hSOD1 and mitoKARS was confirmed using antibodies against human SOD1 and Myc, respectively. *F*, blue native gel on hSOD1/mitoKARS co-expressing cells, immunodetected for mitoKARS with the LysRS antibody and for complex III of the respiratory chain. *G*, nuclear-encoded mitochondrial proteins, Hsp60 (matrix), VDAC (outer membrane), and Tim23 (inner membrane) were analyzed by Western blot to determine mitochondrial protein content in blue native samples shown in *F*.

aggregation of mitoKARS occurs mostly on the external surface of the mitochondrial outer membrane.

To test whether mutant hSOD1 interferes with mitoKARS import, we correlated the amount of mitoKARS associated with mitochondria with that of total cellular mitoKARS. Mitochondrial mitoKARS was normalized by the content of Tim23, a marker of the inner membrane. Total cellular mitoKARS was normalized by the content of the cytosolic protein GAPDH. We find less mitoKARS associated with mitochondria in mutant hSOD1 cells, as compared with cells expressing WT hSOD1 (Fig. 3, *B* and *C*).

To determine whether reduced mitoKARS import affects normal mitochondrial protein synthesis, we performed a [^{35}S]methionine pulse labeling of mitochondrial DNA (mtDNA) synthesized proteins in cells expressing KARS and WT or G85R hSOD1. We find a generalized decrease in mitochondrial protein synthesis in cells expressing G85R hSOD1 (Fig. 3*D*). Quantification by phosphorimaging of selected labeled mitochondrial peptides revealed approximately a 25% reduction in the translation of ND1, ND5, and A6 (data not shown). The same samples were also analyzed by Western blot to detect GAPDH and Tim23 as protein loading controls and hSOD1 and mitoKARS to confirm transgene expression (Fig. 3*E*). These results suggest that mutant hSOD1 interaction affects mitochondrial function through an impairment of protein synthesis. Blue native gel electrophoresis to detect assembled mitochondrial respiratory chain complexes detected a defect in complex III, which paralleled a reduction in the content of dimeric mitoKARS in cells expressing G85R mutant hSOD1 (Fig. 3*F*). The reduction in complex III is likely the result of decreased synthesis of cytochrome *b*, which is mtDNA-encoded. We looked at the nuclear encoded mitochondrial proteins VDAC, Tim 23, and Hsp60 by Western blot in the samples used for blue native gels to control for protein loading (Fig. 3*G*).

Nonimported mitoKARS Is Degraded through the Ubiquitin-Proteasome System—The ubiquitin-proteasome system (UPS) has been linked to ALS pathogenesis (reviewed in Ref. 28). Among many other functions, UPS is involved in regulating mitochondrial protein import (29), and mutations in components of the UPS can affect mitochondrial morphology in yeast (30, 31). In addition, proteins involved in tRNA import, including the precursor of mitoKARS (pre-MSK1p), interact with components of the UPS, and proteasome inhibition decreases mitochondrial tRNA import (32). Because mitoKARS appears to be poorly imported and aggregates in the presence of mutant SOD1, we tested whether the UPS is involved in degrading nonimported mitoKARS. Treatment with the proteasome inhibitor MG132 increases the unprocessed, nonimported, form of mitoKARS in cells co-expressing hSOD1 and mitoKARS (Fig. 4*A*, *left panels*), whereas cytoKARS content is unchanged (Fig. 4*A*, *right panels*). Because there is no evidence that mitochondria contain a proteasome machinery to degrade mitoKARS after import, this result indicates that the substrate for UPS degradation is nonimported mitoKARS. As expected, the amounts of total ubiquitinated proteins as well as hSOD1 are also increased, confirming UPS inhibition, whereas Tim23, an integral mitochondrial protein, is unaffected. UPS inhibition results in increased interaction between mitoKARS and hSOD1. This increase is markedly more prominent with mutant than with WT SOD1 (Fig. 4*B*), further confirming that misfolded mutant SOD1 interacts preferentially with nonimported mitoKARS. To determine whether mutant SOD1, by decreasing mitoKARS import, increases the levels of ubiquitinated mitoKARS, the cells were subjected to a partial protea-

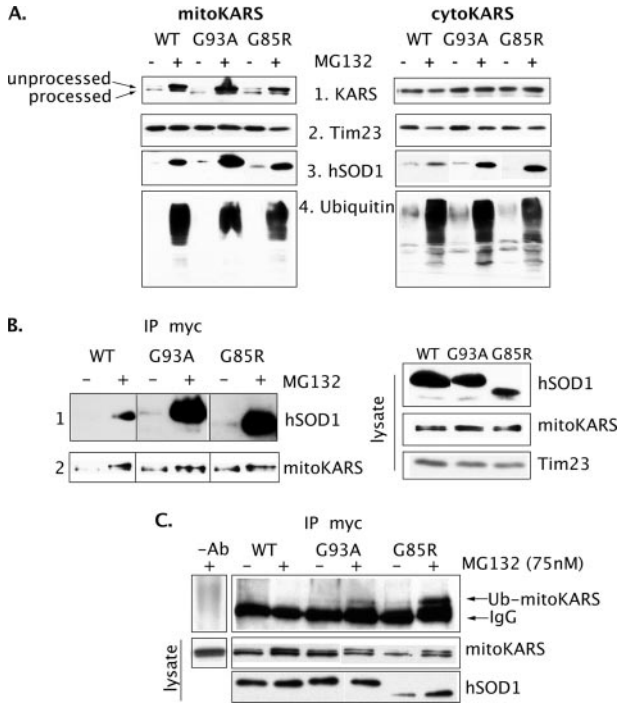

FIGURE 4. **Nonimported mitoKARS is degraded by the ubiquitin-proteasome system.** *A*, COS cells co-transfected with hSOD1 and either cytoKARS or mitoKARS were treated with 20 μM of the proteasome inhibitor MG132 for 16 h. Proteasome inhibition increases the levels of unprocessed mitoKARS (*panel 1*, *left*) but not cytoKARS (*panel 1*, *right*). As expected, hSOD1 (*panels 3*) and total ubiquitinated protein (*panels 4*) levels are also increased, and the mitochondrial inner membrane protein Tim23 is unchanged (*panels 2*). *B*, *left panels*, proteasome inhibition increases the interactions between mutant hSOD1 and mitoKARS, as detected by co-IP of hSOD1 with the Myc antibody (*panel 1*). *Panel 2* shows immunoprecipitated mitoKARS. *Right panels*, expression levels of hSOD1 and mitoKARS in lysates from untreated cells. Tim23 is used as the loading control. *C*, under partial (75%) proteasome inhibition with 75 nM MG132, ubiquitinated mitoKARS (band denoted as *Ub-mitoKARS*) is increased in mutant but not in WT hSOD1 expressing cells (*top panel*). Note that the ubiquitin antibody recognizes the IgG heavy chain from the mouse Myc antibody (band denoted as *IgG*). A negative control IP without Myc primary antibody (*Ab*) is shown in the *first lane*. The *bottom panels* show mitoKARS and hSOD1 expression in cell lysates.

some inhibition (by 75%, as estimated by a fluorogenic assay; data not shown). mitoKARS ubiquitination increases in cells expressing mutant hSOD1, as compared with WT hSOD1 (Fig. 4*C*). Taken together, these results suggest that mutant hSOD1 inhibits mitoKARS import, probably by promoting misfolding and aggregation on the outer surface of mitochondria, and that nonimported mitoKARS becomes a target for UPS degradation in the cytoplasm.

Altered Mitochondrial Morphology and Cell Viability in Cells Expressing mitoKARS and Mutant SOD1—Accumulation of misfolded proteins, such as mitoKARS and mutant SOD1, at the mitochondrial surface may result in pathological changes of mitochondrial structure. We studied mitochondrial morphology in cells co-transfected with mitoKARS and hSOD1 and compared it with controls transfected with GFP targeted to mitochondria (mitoGFP) and hSOD1. All cells expressing hSOD1 in combination with either mitoGFP or mitoKARS were scored as normal or abnormal, based on the morphology of the mitochondrial network. Normal mitochondrial morphology consists of elongated, tubular, and uniformly distributed mitochondria (Fig. 5*A*). Abnormal morphology includes

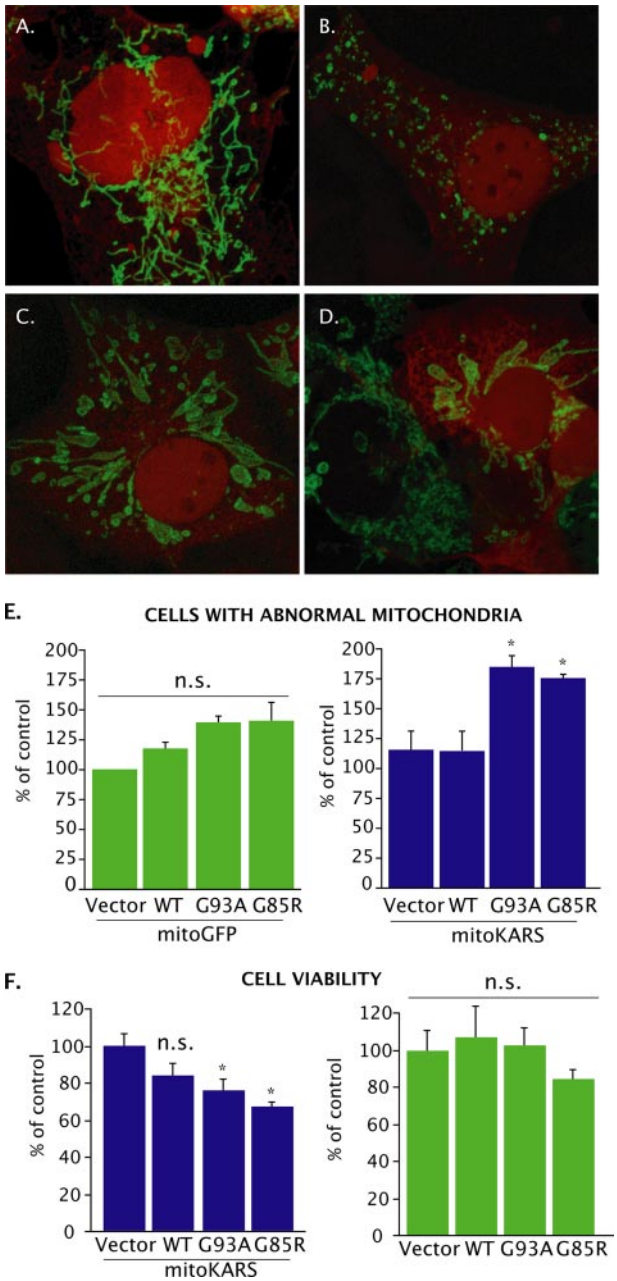

FIGURE 5. **mitoKARS and mutant hSOD1 alter mitochondrial morphology and decrease cell viability.** *A–D*, COS cells expressing hSOD1 (immunostained in *red*) together with mitoKARS (in *green*). Mitochondrial morphological changes were analyzed in cells expressing both constructs; tubular and uniformly distributed mitochondria were scored as normal (*A*, mitoKARS plus WT hSOD1), whereas mitochondria with fragmentation, fusion and clustering, and perinuclear concentration (*B–D*, mitoKARS plus G85R hSOD1) were scored as abnormal. *E*, the changes in number of cells containing abnormal mitochondria are expressed relative to control cells transfected with mitoGFP and empty vector (set at 100%). hSOD1 plus mitoGFP do not alter mitochondrial morphology as compared with controls (*left*), whereas cells transfected with both mutant hSOD1 and mitoKARS (*right*) are significantly more prone to have abnormal mitochondria than control cells. *n.s.*, nonsignificant differences *versus* control; *, $p < 0.01$, $n = 5$ independent experiments. *F*, COS cells were transfected with hSOD1 only (*right panel*) or with hSOD1 and mitoKARS (*left panel*). Cells expressing mutant hSOD1 and mitoKARS show significantly reduced cell viability, whereas hSOD1 expression alone does not cause cell toxicity. The data are expressed as percentages of the values of calcein fluorescence measured in vector controls. *n.s.*, nonsignificant differences *versus* control; *, $p < 0.05$, $n = 10$ independent experiments. In *E* and *F*, differences were determined by analysis of variance followed by Fisher's post-hoc test, and the *error bars* indicate S.E.

fragmented and rounded mitochondria (Fig. 5*B*), clustered and enlarged mitochondria (Fig. 5*C*), or perinuclear clustering of mitochondria (Fig. 5*D*, co-transfected cell on the right side of the micrograph). The proportion of cells containing abnormal mitochondria is not increased significantly by the expression of hSOD1 in conjunction with mitoGFP (Fig. 5*E*, *left panels*). However, mitoKARS expression together with mutant, but not WT hSOD1, results in an increase in the proportion of cells containing abnormal mitochondria (Fig. 5*E*, *right panels*).

We investigated the effects of mitoKARS and hSOD1 co-expression on cell viability. A calcein AM-based assay was used to estimate cell survival 24 h after transfection. Note that the assay measures calcein esterification in all live cells, regardless of expression of the transgene. Therefore, the cell toxicity of mutant hSOD1 plus mitoKARS is underestimated by this approach, because only ~20% of the cells expressed both transgenes, with similar transfection efficiency among all hSOD1 constructs. Nevertheless, co-expression of mitoKARS with mutant hSOD1 results in decreased cell viability (Fig. 5*F*, *left panels*), whereas mutant hSOD1 without mitoKARS has no statistically significant effect (Fig. 5*F*, *right panels*).

DISCUSSION

Cellular and transgenic mouse models of familial ALS expressing mutant SOD1 show mitochondrial degeneration resulting in loss of membrane potential, ATP production, and calcium handling (14). However, the mechanisms whereby mutant SOD1 damages mitochondrial function remain to be identified. One potential mechanism involves aberrant protein interactions between mutant SOD1 and other proteins. Examples of this type of interactions have been previously reported, such as the selective binding of mutant SOD1 to the anti-apoptotic protein Bcl-2 (16), although another group did not confirm this interaction (33). Bcl-2 is probably only one of the potentially many mitochondrial proteins that may be affected by aberrant interaction with mutant hSOD1, which has a strong tendency to misfold and aggregate.

In this study we focused on KARS, because it was found to interact predominantly with mutant SOD1 by a yeast interaction trap system (17). KARS localizes in motor neurons with a distribution pattern similar to SOD1, but the biological relevance of the abnormal interactions between mutant SOD1 and KARS have not yet been explored. tRNA synthetases are involved in aminoacylation of specific tRNAs during protein translation of nuclear DNA encoded proteins in the cytosol and mtDNA-encoded proteins in the mitochondrial matrix. Furthermore, the precursor of mitoKARS is thought to allow for the mitochondrial import of cytosolic tRNAlys (32). The mitochondrial and cytosolic isoforms of KARS are derived from a single gene; mitoKARS mRNA contains exon 2, which encodes for the mitochondrial targeting signal, whereas cytoKARS mRNA excludes exon 2 by an exon skipping mechanism (18). It is remarkable that mutations in the glycyl-tRNA synthetase, whose cytosolic and mitochondrial isoforms are also encoded by a single gene, are responsible for dominantly inherited forms of Charcot Marie Tooth neuropathy (34). This emerging evidence suggests that KARS and other tRNA synthetases can play an important role in disease pathogenesis (35).

We find that in mammalian cells mitoKARS interacts with mutant more abundantly than with WT SOD1, whereas cytoKARS does not interact (Fig. 2). The physiological reasons behind the interaction between mitoKARS and SOD1 are unknown. Nevertheless, it could be speculated that mitoKARS and SOD1 interaction is somehow involved in mitochondrial protein import. Although such a novel function has never been documented before for any of tRNA synthetases, novel noncanonical functions have been recently described for several of them (36). For example, KARS was shown to be involved in regulation of transcription factors in mast cells (37), and mitoKARS has been implicated in mitochondrial import of cytosolic tRNAs (32).

Misfolded SOD1 at the mitochondrial outer surface prevents the mitoKARS precursor (*i.e.* the unprocessed protein) from being readily imported through the translocator and results in the accumulation of nonimported mitoKARS (Fig. 3). Our results do not address directly whether mutant SOD1 interacts with the monomeric or the dimeric form of mitoKARS. However, because most of the interaction appears to occur prior or during import of mitoKARS into mitochondria, which requires the protein to be unfolded and monomeric, it is highly likely that the interaction with mutant SOD1 involves the monomer of KARS. The nature of the molecular interactions between mitoKARS and mutant SOD1 remains to be fully elucidated. However, it is likely that the two proteins reside in close proximity at the surface of mitochondria, where they may interact through covalent disulfide or electrostatic bonds, forming hetero-oligomers or large, multi-protein, molecular aggregates. Another potential mechanism whereby mutant SOD1 may impair mitochondrial protein import is by decreasing the pool of cytosolic chaperones. In fact, mutant SOD1 has been shown to interact with cytosolic chaperones, such as Hsp70, which is crucial for maintaining precursor proteins in the unfolded state and delivering them to the translocator machinery of the outer membrane (38).

The aberrant interaction between mutant SOD1 and mitoKARS may result in multiple noxious effects that can destabilize mitochondria. First, mutant SOD1 aggregates in mitochondria both *in vivo* and *in vitro* (6, 7) (Fig. 2), probably involving several other mitochondrial proteins, such as the mitoKARS precursor. The accumulation of aberrant high molecular weight protein structures on the surface of mitochondria may contribute to damage by sequestering proteins necessary for maintaining mitochondrial integrity and dynamics, such as, for example, components of the machineries involved in mitochondrial protein translocation, fusion, fission, and transport.

Second, abnormal interactions with mutant SOD1 may reduce the amount of mature mitoKARS available for mitochondrial protein synthesis and the precursor for tRNAlys import. We observed that a decrease in mitoKARS import in mitochondria in the presence of mutant SOD1 corresponded to impaired synthesis of mtDNA-encoded peptides (Fig. 3).

In cells where only endogenous mitoKARS is present, impaired mitochondrial protein synthesis associated with mutant SOD1 may contribute to mitochondrial dysfunction. Indeed, mitochondrial structural and functional defects have

been observed in motor neuron-like NSC-34 cells stably expressing mutant SOD1, in the absence of mitoKARS overexpression (39, 40). Furthermore, in mutant SOD1 transgenic mice there is a mitochondrial respiratory chain defect involving mtDNA-encoded enzymes (4, 12, 41). Neurons are likely to be highly sensitive to this type of mitochondrial damage, because significant defects were not observed *in vivo* in non-neural tissues of mutant SOD1 transgenic mice or in cultured COS cells expressing mutant SOD1 without mitoKARS (Fig. 5).

Another potential mechanism, whereby the loss of mitoKARS could result in destabilization of mtDNA-encoded proteins, is suggested by the "sticky mutation" in another tRNA synthetase, alanyl-tRNA synthetase (42). In mice, sticky mutant alanyl-tRNA synthetase, lacking the function of deacylating mischarged tRNAala, results in amino acid misincorporation in nascent peptides and causes neuronal degeneration. Impaired mitoKARS import could result in a similar loss of quality control in mitochondrial protein and their misfolding and aggregation, leading to mitochondrial dysfunction. Further studies will be needed to test this hypothesis by assessing the editing functions of mitoKARS in mutant SOD1 mitochondria.

In summary, our results indicate that aberrant interactions with mutant SOD1 result in misfolded mitoKARS that accumulates on the outside of mitochondria and is sent to the UPS for degradation. mitoKARS interactions with mutant SOD1 are associated with impaired mtDNA-encoded protein synthesis and aberrant mitochondrial morphology, which ultimately cause a loss of cell viability. We suggest that mitoKARS is representative of a potentially large group of proteins, whose interaction with mutant SOD1 alters mitochondrial import and contributes to mitochondrial dysfunction in familial ALS.

Acknowledgments—We thank Drs. L. Kleiman and S. Cen (Lady Davis Institute for Medical Research/Jewish General Hospital, Montreal, Canada) for kindly providing the LysRS antibody against human KARS.

REFERENCES

1. Higgins, C. M., Jung, C., Ding, H., and Xu, Z. (2002) *J. Neurosci.* **22,** RC215
2. Jaarsma, D., Rognoni, F., van Duijn, W., Verspaget, H. W., Haasdijk, E. D., and Holstege, J. C. (2001) *Acta Neuropathol.* **102,** 293–305
3. Liu, J., Lillo, C., Jonsson, P. A., Velde, C. V., Ward, C. M., Miller, T. M., Subramaniam, J. R., Rothstein, J. D., Marklund, S., Andersen, P. M., Brannstrom, T., Gredal, O., Wong, P. C., Williams, D. S., and Cleveland, D. W. (2004) *Neuron* **43,** 5–17
4. Mattiazzi, M., D'Aurelio, M., Gajewski, C. D., Martushova, K., Kiaei, M., Beal, M. F., and Manfredi, G. (2002) *J. Biol. Chem.* **277,** 29626–29633
5. Okado-Matsumoto, A., and Fridovich, I. (2001) *J. Biol. Chem.* **276,** 38388–38393
6. Vijayvergiya, C., Beal, M. F., Buck, J., and Manfredi, G. (2005) *J. Neurosci.* **25,** 2463–2470
7. Deng, H. X., Shi, Y., Furukawa, Y., Zhai, H., Fu, R., Liu, E., Gorrie, G. H., Khan, M. S., Hung, W. Y., Bigio, E. H., Lukas, T., Dal Canto, M. C., O'Halloran, T. V., and Siddique, T. (2006) *Proc. Natl. Acad. Sci. U. S. A.* **103,** 7142–7147
8. Dal Canto, M. C., and Gurney, M. E. (1995) *Brain Res.* **676,** 25–40
9. Wong, P. C., Pardo, C. A., Borchelt, D. R., Lee, M. K., Copeland, N. G., Jenkins, N. A., Sisodia, S. S., Cleveland, D. W., and Price, D. L. (1995) *Neuron* **14,** 1105–1116
10. Kong, J., and Xu, Z. (1998) *J. Neurosci.* **18,** 3241–3250
11. Jung, C., Higgins, C. M., and Xu, Z. (2002) *J. Neurosci. Methods* **114,** 165–172
12. Kirkinezos, I. G., Bacman, S. R., Hernandez, D., Oca-Cossio, J., Arias, L. J., Perez-Pinzon, M. A., Bradley, W. G., and Moraes, C. T. (2005) *J. Neurosci.* **25,** 164–172
13. Damiano, M., Starkov, A. A., Petri, S., Kipiani, K., Kiaei, M., Mattiazzi, M., Flint Beal, M., and Manfredi, G. (2006) *J. Neurochem.* **96,** 1349–1361
14. Hervias, I., Beal, M. F., and Manfredi, G. (2006) *Muscle Nerve* **33,** 598–608
15. Okado-Matsumoto, A., and Fridovich, I. (2002) *Proc. Natl. Acad. Sci. U. S. A.* **99,** 9010–9014
16. Pasinelli, P., Belford, M. E., Lennon, N., Bacskai, B. J., Hyman, B. T., Trotti, D., and Brown, R. H., Jr. (2004) *Neuron* **43,** 19–30
17. Kunst, C. B., Mezey, E., Brownstein, M. J., and Patterson, D. (1997) *Nat. Genet.* **15,** 91–94
18. Tolkunova, E., Park, H., Xia, J., King, M. P., and Davidson, E. (2000) *J. Biol. Chem.* **275,** 35063–35069
19. Rizzuto, R., Brini, M., Pizzo, P., Murgia, M., and Pozzan, T. (1995) *Curr. Biol.* **5,** 635–642
20. Gurney, M. E., Pu, H., Chiu, A. Y., Dal Canto, M. C., Polchow, C. Y., Alexander, D. D., Caliendo, J., Hentati, A., Kwon, Y. W., Deng, H. X., and et al. (1994) *Science* **264,** 1772–1775
21. Pallotti, F., and Lenaz, G. (2001) *Methods Cell Biol.* **65,** 1–35
22. Cen, S., Javanbakht, H., Kim, S., Shiba, K., Craven, R., Rein, A., Ewalt, K., Schimmel, P., Musier-Forsyth, K., and Kleiman, L. (2002) *J. Virol.* **76,** 13111–13115
23. D'Aurelio, M., Gajewski, C. D., Lenaz, G., and Manfredi, G. (2006) *Hum. Mol. Genet.* **15,** 2157–2169
24. Chomyn, A. (1996) *Methods Enzymol.* **264,** 197–211
25. Mirande, M., Le Corre, D., and Waller, J. P. (1985) *Eur. J. Biochem.* **147,** 281–289
26. Robinson, J. C., Kerjan, P., and Mirande, M. (2000) *J. Mol. Biol.* **304,** 983–994
27. Wang, J., Xu, G., and Borchelt, D. R. (2002) *Neurobiol. Dis.* **9,** 139–148
28. Kabashi, E., and Durham, H. D. (2006) *Biochim. Biophys. Acta* **1762,** 1038–1050
29. Pearce, D. A., and Sherman, F. (1997) *J. Biol. Chem.* **272,** 31829–31836
30. Fisk, H. A., and Yaffe, M. P. (1999) *J. Cell Biol.* **145,** 1199–1208
31. Rinaldi, T., Pick, E., Gambadoro, A., Zilli, S., Maytal-Kivity, V., Frontali, L., and Glickman, M. H. (2004) *Biochem. J.* **381,** 275–285
32. Brandina, I., Smirnov, A., Kolesnikova, O., Entelis, N., Krasheninnikov, I. A., Martin, R. P., and Tarassov, I. (2007) *FEBS Lett.* **581,** 4248–4254
33. Gould, T. W., Buss, R. R., Vinsant, S., Prevette, D., Sun, W., Knudson, C. M., Milligan, C. E., and Oppenheim, R. W. (2006) *J. Neurosci.* **26,** 8774–8786
34. Antonellis, A., Ellsworth, R. E., Sambuughin, N., Puls, I., Abel, A., Lee-Lin, S. Q., Jordanova, A., Kremensky, I., Christodoulou, K., Middleton, L. T., Sivakumar, K., Ionasescu, V., Funalot, B., Vance, J. M., Goldfarb, L. G., Fischbeck, K. H., and Green, E. D. (2003) *Am. J. Hum. Genet.* **72,** 1293–1299
35. Park, S. G., Schimmel, P., and Kim, S. (2008) *Proc. Natl. Acad. Sci. U. S. A.* **105,** 11043–11049
36. Park, S. G., Ewalt, K. L., and Kim, S. (2005) *Trends Biochem. Sci.* **30,** 569–574
37. Yannay-Cohen, N., and Razin, E. (2006) *Mol. Cells* **22,** 127–132
38. Young, J. C., Agashe, V. R., Siegers, K., and Hartl, F. U. (2004) *Nat. Rev. Mol. Cell. Biol.* **5,** 781–791
39. Menzies, F. M., Cookson, M. R., Taylor, R. W., Turnbull, D. M., Chrzanowska-Lightowlers, Z. M., Dong, L., Figlewicz, D. A., and Shaw, P. J. (2002) *Brain* **125,** 1522–1533
40. Raimondi, A., Mangolini, A., Rizzardini, M., Tartari, S., Massari, S., Bendotti, C., Francolini, M., Borgese, N., Cantoni, L., and Pietrini, G. (2006) *Eur. J. Neurosci.* **24,** 387–399
41. Son, M., Puttaparthi, K., Kawamata, H., Rajendran, B., Boyer, P. J., Manfredi, G., and Elliott, J. L. (2007) *Proc. Natl. Acad. Sci. U. S. A.* **104,** 6072–6077
42. Lee, J. W., Beebe, K., Nangle, L. A., Jang, J., Longo-Guess, C. M., Cook, S. A., Davisson, M. T., Sundberg, J. P., Schimmel, P., and Ackerman, S. L. (2006) *Nature* **443,** 50–55